JPET Fast Forward. Published on March 30, 2017 as DOI: 10.1124/jpet.116.239574
This article has not been copyedited and formatted. The final version may differ from this version.

A genomic DNA reporter screen identifies squalene synthase inhibitors which act cooperatively with statins to upregulate the low-density lipoprotein receptor

Alastair G. Kerr, Lawrence C.S. Tam, Ashley B. Hale, Milena Cioroch, Gillian Douglas, Sarina Agkatsev, Olivia Hibbitt, Joseph Mason, James Holt-Martyn, Carole J. R. Bataille, Graham M. Wynne, Keith M. Channon, Angela J. Russell, and Richard Wade-Martins

Department of Physiology, Anatomy and Genetics, University of Oxford, Oxford, UK; (AK., LT., MC., SA., OH., JH-M., RW-M)

Division of Cardiovascular Medicine, British Heart Foundation Centre of Research Excellence, University of Oxford, John Radcliffe Hospital, Oxford OX3 9DU, UK (AH., GD., KC)

Department of Chemistry, Chemistry Research Laboratory, University of Oxford, Mansfield Road, Oxford, UK (JM., CB., GW., AR)

Department of Pharmacology, University of Oxford, Mansfield Road, Oxford, UK (AR)

Novel small molecules which upregulate the LDLR

Joint corresponding authors

Correspondence should be addressed to Richard Wade-Martins, MA, DPhil, Le Gros Clark Building, Department of Physiology, Anatomy and Genetics, University of Oxford, South Parks Road, Oxford, OX1 3QX United Kingdom. E-mail: richard.wade-martins@dpag.ox.ac.uk Telephone number: +441865 282837

Other corresponding author

Angela Russell, MChem, DPhil, Department of Chemistry, Chemistry Research Laboratory, University of Oxford, Mansfield Road, Oxford OX1 3TA, UK; Department of Pharmacology, University of Oxford, Mansfield Road, Oxford OX1 3QT, UK. Email: angela.russell@chem.ox.ac.uk. Telephone number: +441865 275 643 (Chemistry) /271 883 (Pharmacology)

Text pages: 34

Number of tables: 0

Number of figures: 6

References: 32

Abstract word count: 225

Introduction word count: 649

Discussion word count: 1079

Section: Drug Discovery and Translational Medicine

Non-standard abbreviations – Familial Hypercholesterolaemia (FH), 3-hydroxy-3-methylglutaryl coenzyme A reductase (HMGCR), Low-density Lipoprotein Receptor (LDLR), Squalene Synthase (SQS)

Abstract:

Hypercholesterolaemia remains one of the leading risk factors for the development of cardiovascular disease. Many large double-blind studies have demonstrated that lowering LDL-cholesterol using a statin can reduce the risk of having a cardiovascular event by ~30%. However, despite the success of statins, some patient populations are unable to lower their LDL-cholesterol to meet the targeted lipid levels, due to compliance or potency issues. This is especially true for heterozygous familial hypercholesterolaemia (heFH) patients who may require additional upregulation of the Low-Density Lipoprotein Receptor (LDLR) to reduce LDL-cholesterol levels below those achievable with maximal dosing of statins. Here we identify a series of small molecules from a genomic DNA reporter screen which upregulate the LDLR in mouse and human liver cell lines at nanomolar potencies (EC_{50}: 39 nM). Structure-activity relationship studies carried out on the lead compound (compound OX03771) led to the identification of compound OX03050, which had similar potency (EC_{50}: 26 nM), but a much-improved pharmacokinetic profile and showed *in vivo* efficacy. Compound OX03050 and OX03771 were found to inhibit squalene synthase, the first committed step in cholesterol biosynthesis. These squalene synthase inhibitors were shown to act cooperatively with statins to increase LDLR expression *in vitro.* Overall, we have demonstrated here a novel series of small molecules with the potential to be further developed to treat patients either alone, or in combination with statins.

JPET Fast Forward. Published on March 30, 2017 as DOI: 10.1124/jpet.116.239574
This article has not been copyedited and formatted. The final version may differ from this version.

Introduction

Cardiovascular disease remains one of the largest health and economic burdens in the world. High circulating levels of low-density lipoprotein cholesterol (LDL-cholesterol) remains one of the biggest risk factors for cardiovascular disease, as it leads to the accelerated development of atherosclerosis and progression into coronary heart disease (Lusis 2000). The front-line pharmacotherapies to lower LDL-cholesterol are the 3-hydroxy-3-methylglutaryl coenzyme A reductase (HMGCR) inhibitors, known as statins. Statins have been very successful in primary and secondary prevention of coronary heart disease (Pedersen 1994; Shepherd *et al.* 1995), with many large randomised control trials demonstrating a reduction in cardiovascular disease directly correlated with lowering of LDL-cholesterol (Sniderman *et al.* 2012). Despite their success some patients either fail to achieve their lipid goal or experience intolerable side effects such as myotoxicity (Moßhammer *et al.* 2014), leading to them discontinuing taking statin medication. However, there has been some controversy regarding the rate of adverse events related to statins, with some large randomised controlled trials describing no difference in reported side effects compared with placebo (Ridker et al. 2008). The rate of myopathy in these trials is usually around 3% (Bays 2006), although the rate of statin intolerance in the general population may be as high as 10-15% (Grundy 2002; Joy and Hegele 2009). These side effects are much more common in patients on the maximum dose of statins, so therapies which could be used in conjunction with a reduced dose of statins to lower LDL-cholesterol, may increase compliance and help more patients achieve their targeted lipid levels.

Squalene synthase is involved in the same cholesterol biosynthesis pathway as HMGCR but represents the first committed step in cholesterol synthesis. Statins act

upstream of squalene synthase and so also inhibit the production of other non-steroidal isoprenoid molecules, such as isopentenyl adenine (protein synthesis), coenzyme Q_{10} (mitochondrial respiration) and dolichol (glycosylation), a consequence that has been linked to their side effects (Bitzur *et al.* 2013) (Marcoff and Thompson 2007). Squalene synthase inhibitors have been shown to upregulate the low-density lipoprotein receptor (LDLR) like statins, but without inhibiting the production of these other intermediates (Davidson 2007). In fact squalene synthase inhibitors administered with statins were shown to have a protective effect on statin-induced myotoxicity (Nishimoto *et al.* 2007). Many squalene synthase inhibitors have shown similar or greater anti-hyperlipidemic effects than statins (Ugawa *et al.* 2000)(Nishimoto *et al.* 2003) and they continue to be developed as promising lipid lowering agents to complement statins (Ichikawa *et al.* 2013). The squalene synthase inhibitor lapaquistat acetate reached phase II/III clinical trials (Stein *et al.* 2011) where it was generally well tolerated and significantly reduced LDL-cholesterol. When used in conjunction with statins, lapaquistat acetate reduced LDL-cholesterol by a further 19%, when compared with statin monotherapy. Unfortunately, lapaquistat acetate was withdrawn due to hepatotoxicity seen in two patients receiving a high dose. It was never established whether the hepatotoxicity was a result of off-target effects of lapaquistat acetate, or through inhibition of squalene synthase. Interestingly, squalene synthase knockout mice exhibit only a modest liver injury despite complete loss of enzyme function, thought to result from a build-up of the squalene synthase substrate farnesyl diphosphate (FPP) (Nagashima *et al.* 2015). Treatment with a statin would alleviate this build up, similar to that already observed using this combination of inhibitors to prevent non-sterol isoprenoid depletion associated with statins (Wasko *et al.* 2011).

JPET Fast Forward. Published on March 30, 2017 as DOI: 10.1124/jpet.116.239574
This article has not been copyedited and formatted. The final version may differ from this version.

Here we present a set of novel stilbenoid-derived small molecules which can upregulate the LDLR at the mRNA and protein level with nanomolar potencies. We carried out preliminary structure activity relationship studies to improve the efficacy and pharmacokinetic profile. The mechanism of action was established through enzymatic assays and supported by *in silico* modelling. We demonstrate that these small molecules are able to drive expression of the human *LDLR* promoter *in vivo* and when dosed in combination with statins give a much greater effect than can be seen with either inhibitor alone.

Methods

Cell culture

Human Hep3B cells were a kind gift from Dr Zoe Holloway. Mouse hepatoma Hepa 1–6 cells were a kind gift from Dr Natalia Sacilotto. Both cell lines were grown in Dulbecco's modified Eagle's medium supplemented with 10% fetal bovine serum (FBS), 1% penicillin/ streptomycin, 1% L-glutamine, in a 5% CO2 incubator at 37ºC. For mRNA analysis Hep3B cells were seeded in 24-well plates. For Western blot analysis Hepa1-6 cells were seeded in 6-well plates. After 24 h cells were changed to Dulbecco's modified Eagle's medium supplemented with 5% lipoprotein deficient serum (LDPS), 1% penicillin/ streptomycin, 1% L-glutamine.. CHO WT cells transfected with *pLDLR-Luc* (CHO-*pLDLR-Luc*) establishing a clonal cell line, were grown in HamsF-12 medium supplemented with 10% fetal bovine serum (FBS), 1% penicillin/ streptomycin, 1% L-glutamine, in a 5% CO2 incubator at 37°C. CHO-*pLDLR-Luc* were seeded in 24-well plates. After 24 h, cells were changed to HamsF-12 supplemented with 5% LDPS, 1% penicillin/ streptomycin and 1% L-glutamine. compounds, Simvastatin (Sigma, St Louis, MO) and Pravastatin (Sigma) dissolved in DMSO and Cholesterol (Sigma) and 25-Hydroxycholesterol (Sigma) dissolved in ethanol were added 24 h after.

Luciferase assay

CHO-p*LDLR-Luc* cells were lysed 48 h after compound treatment using lysis buffer containing 1% Triton X-100. 2 mM ATP, 2 mM DTT and 1 mM D-Luciferin were added to the lysate in luciferase assay buffer containing 15 mM MgSO4, 15 mM KPO4 and 4 mM EGTA at pH 7.8. Luciferase activity was quantified on a Dynex Technologies MLX 96 well plate luminometer (Dynex Technologies, Chantilly, VA). Protein concentration was determined using a BCA Protein assay kit with Bovine Serum

JPET Fast Forward. Published on March 30, 2017 as DOI: 10.1124/jpet.116.239574
This article has not been copyedited and formatted. The final version may differ from this version.

Albumin to generate a standard curve. Luciferase activity was normalized to total protein within each well.

qRT-PCR

RNA was extracted from Hep3B cells 24 h after compound treatment, using RNeasy mini kit (Qiagen, Valencia, CA) according to manufacturer's protocol. cDNA was reverse transcribed from 1 µg of total RNA using random primers, SuperScript III Reverse Transcriptase and RNaseOUT™ recombinant RNase inhibitor. Quantitative Real-time PCR was performed on a StepOnePlus Real-Time PCR system, with SYBR Green PCR Master Mix according to the manufacturer's protocol. Gene and species specific primers were used for LDLR: Forward gacagatgcgaaagaaacga, Reverse acagacaagcacgtctcctg. B-Actin: Forward agcgcggctacagcttca, Reverse cgtagcacagcttctccttaatgtc. B-Actin was used as a housekeeper gene and all samples were run in triplicates. ΔΔCt was calculated and used for quantification.

Western blot analysis

Hepa1-6 cells were lysed 48 h after compound treatment using lysis buffer containing 0.5% NP40. Protein concentration was determined using a BCA Protein assay kit with Bovine Serum Albumin to generate a standard curve. 15 µg total protein was heated at 90ºC for 5 minutes then loaded into each well and run on a 10% SDS-polyacrylamide. Samples were transferred to a PVDF membrane cut and stained with LDLR (ab30532, Abcam, Cambridge, MA) or β-actin (ab8226, Abcam) primary antibody overnight at 4ºC. Membranes were then incubated with horseradish peroxidase-conjugated polyclonal rabbit IgG secondary antibody (Abcam). All blots were developed using enhanced chemiluminescent substrate kit (Pierce, Thermo Scientific, Waltham, MA) and exposed to Fugi X-ray films in a dark-room facility.

JPET Fast Forward. Published on March 30, 2017 as DOI: 10.1124/jpet.116.239574
This article has not been copyedited and formatted. The final version may differ from this version.

Protein band intensities were quantified by scanning with Canon M550 Scanner and analysed using ImageJ.

Adenylate kinase assay

Cell media was aspirated from wells of CHO-p*LDLR-Luc* cells treated with compounds for 48 hours. Adenylate kinase concentration present in the media was quantified using Bioluminescence Cytotoxicity Assay Kit (MBL, Woburn, MA) as per manufactures instructions. Luciferase activity was quantified on a Dynex Technologies MLX 96 well plate luminometer.

Squalene synthase activity assay

Squalene synthase activity was assessed as described earlier (Amin *et al.* 1992). Briefly each assay was in 1 mL of assay buffer (50 mM phosphate buffer, pH 7.4 containing 10 mM $MgCl_2$) containing 0.5 mM NADPH, 12 µg of human liver microsomes and compound or vehicle (DMSO) alone in 16x100mm glass screw cap tubes. All components were allowed to equilibrate for 10 minutes at 37^{o}C before addition of [^{3}H]-FPP (50 nM 0.045 Ci/mmol) (Perkin Elmer, Wokingham, United Kingdom) for a further 10 minutes at 37°C. The reaction was stopped by the addition of 1 mL of 15% KOH dissolved in EtOH. Tubes were incubated at 65^{o}C for 30 minutes then 5 mL of petroleum ether was added and shaken for 10 minutes. The lower aqueous phase was frozen and the upper organic phase transferred to clean glass tubes containing 2 mL distilled water. 1.5 mL of the upper organic phase was removed and counted with 3 mL of scintillation liquid on a Tri-Carb 2800 TR Liquid Scintillation Analyzer.

JPET Fast Forward. Published on March 30, 2017 as DOI: 10.1124/jpet.116.239574
This article has not been copyedited and formatted. The final version may differ from this version.

Animals and treatment protocols

Maintenance of animals and animal experiments were carried out in accordance with the UK Home Office regulations under the Animals (Scientific Procedures) Act (ASPA) of 1986. Animals had access to food and water ad libitum. All mice were fed a chow diet (Global 16% Protein Rodent Diet, TD.2016, Harlan-Teklad) and maintained at 22°C and 60 – 70% humidity, with a regular 12 h light-dark cycle. Male MF-1 and CD-1 mice were ordered in from Charles River between 21-25 g.

Plasma concentration analysis of compound OX03050 using HPLC

CD-1 male mice were administered with compound OX03050 (40 mg/kg) or vehicle via the intraperitoneal route. Mice were then euthanized at 5, 10, 30, 180 and 360 minutes post compound delivery and plasma was harvested for HPLC analysis. A standard curve was made up of known concentrations spiked into plasma and ran alongside unknown drug concentration samples each time. To make the standard curve known compound OX03050 concentrations were spiked into drug free plasma. Acetonitrile was added to each sample in a 1:8 ratio, samples were shaken for 15 minutes, before being spun at 13,000 rpm for 15 minutes at 4°C. 200 µL of the supernatant was run on a Waters 600 controller HPLC machine with a C18 reverse phase column (Waters), with a linear gradient mobile phase starting at 20:1 H_2O with 0.1% TFA: Acetonitrile with 0.1% TFA rising to 1:20 H_2O with 0.1% TFA: Acetonitrile with 0.1% TFA over 7 minutes at a flow rate of 1.5 mL/min.

Hydrodynamic delivery

Mice weighing between 18-35 g received hydrodynamic tail-vein injections of plasmid DNA as described (Liu, Song and Liu 1999). Animals were anaesthetized with isoflurane and body temperature was maintained using a heating pad. 50 µg of

JPET Fast Forward. Published on March 30, 2017 as DOI: 10.1124/jpet.116.239574
This article has not been copyedited and formatted. The final version may differ from this version.

plasmid DNA was resuspended in TransIT-EE Hydrodynamic Delivery Solution (Mirus, Madison, WI), to a total volume equivalent to 10% of the mouse's total body weight. Delivery of the plasmid was administered via the tail-vein with an injection time between 8-14 seconds depending on the weight of the mouse. Animals were allowed to recover and left for the appropriate amount of time before sacrifice.

In vivo luciferase assay to assess efficacy of compounds

All mice were blinded, separated into treatment groups and assigned a random number, images were taken not knowing which number belonged to which experimental group. Mice 5 days post hydrodynamic delivery had 150 µL of a 15mg/mL D-Luciferin solution delivered via the intraperitoneal (I.P) route, before being anaesthetized using Isoflurane. Following a 5 minute incubation period, mice were placed inside the chamber of an IVIS-100 luciferase imaging camera (Caliper Life Sciences, Waltham, MA) and imaged with a 2 minute exposure time. Mice were dosed 8, 24 and 32 h after acquiring the baseline image with either compound OX03050 (40 mg/kg), vehicle alone or Pravastatin (600 mg/kg), an uninjected group was also included as a control. 48 h on from the first image the mice were imaged under the exact same conditions as before. Images were analysed using LivingImage software (Caliper Life Sciences).

Results

Identification of novel molecules that drive expression of the human LDLR promoter via a mechanism distinct from statins

A Chinese hamster ovary (CHO) clonal cell line was developed (CHO-p*LDLR-Luc*) which contains a 10 kb genomic DNA human low-density lipoprotein receptor (*LDLR*) promoter element driving luciferase. The p*LDLR-Luc* construct has been previously shown to contain the necessary elements for physiological regulation of expression of the *LDLR* locus (Hibbitt *et al.* 2010). To identify compounds which could upregulate expression of the *LDLR* we focused our screening efforts by selecting compounds *in silico* with scaffolds reminiscent of known gene transcription modulators, for example sterols and steroid-like structures. We refined our in-house compound collection to 216 small molecules which we screened at a single concentration (20 µM) in the CHO-p*LDLR-Luc* cell line. Compounds 49 (OX03771), 50 and 51 gave the greatest increase in luciferase activity compared to the vehicle treated control (Figure 1A). This series of compounds was of interest due to their similarity in structure to sterols (Figure 1B), as shown in the overlay of compound OX03771 with cholesterol (Figure 1C). Authentic samples of the three initial hits were synthesized and tested for a dose-dependent response: compound OX03771 was determined to be the most potent (EC_{50} = 39 nM ± 29 SEM, Figure 2A). Hep3B cells were transfected with a p*CMV-Luc* plasmid and treated with compound OX03771 (Supplementary Figure S1A). No significant difference was seen between vehicle-treated or compound OX03771-treated cells expressing p*CMV-Luc*, ruling out compound OX03771 causing an increase in luciferase activity through stabilising or interacting with D-luciferin or luciferase, a commonly observed artefact in these reporter assays (Thorne *et al.* 2012). To confirm compound OX03771 was not itself contributing to the luminescent readout, untransfected Hep3B cells were treated with vehicle or compounds, with no increase

JPET Fast Forward. Published on March 30, 2017 as DOI: 10.1124/jpet.116.239574
This article has not been copyedited and formatted. The final version may differ from this version.

in luminescence detected above untreated cells (Supplementary Figure S1B). An adenylate kinase activity assay carried out on cell culture medium, a measure of cytotoxicity, demonstrated a favourable safety profile of compound OX03771 with only the 10 µM dose showing an increase compared to vehicle treated control cells (Supplementary Figure S1C). The cytotoxicity observed at 10 µM with compound OX03771 correlates with the drop off in luciferase activity observed in the dose-response curve at the same concentration.

Compound OX03771 upregulates the LDLR at the mRNA and protein level

Human and mouse hepatocyte cell lines were treated with compound OX03771 to determine if it could upregulate LDLR mRNA and protein. The EC_{50} dose established in the CHO-p*LDLR-Luc* assay (39 nM) was chosen along with doses 10-fold above and below (Figure 2A). Hep3B cells were treated with compound OX03771, cholesterol (negative control) or a statin (positive control). Compound OX03771 gave a dose-dependent increase at the mRNA level with a significant increase at 390 nM (Figure 2B). To confirm the increase in *LDLR* mRNA resulted in upregulation of the LDLR protein, Hepa1-6 cells were treated with the same concentrations of compound OX03771 (Figure 2C). Compound OX03771 caused a significant upregulation of the LDLR protein compared to vehicle treated control cells at 390 nM similar to that of Simvastatin (Figure 2D).

Compound OX03050 is a more potent analogue of compound OX03771 with improved pharmacokinetic properties

Compound OX03771 was found to have a half-life of less than 5 minutes when incubated with mouse liver microsomes and quantified using liquid chromatography–mass spectrometry (LC-MS) (Supplementary Figure 2A-B). To improve the efficacy, *in vitro* ADME and pharmacokinetic profile of compound OX03771, analogues were

JPET Fast Forward. Published on March 30, 2017 as DOI: 10.1124/jpet.116.239574
This article has not been copyedited and formatted. The final version may differ from this version.

made and their efficacy tested in the CHO-p*LDLR-Luc* clonal cell line (Figure 3). Microsomal incubation of selected analogues was also undertaken to assess metabolic stability. Compound OX03771 was conceptually split into four key regions (Figure 3), the two aromatic rings in the stilbene (Red (A) and Pink (C) rectangles) the carbon-carbon double bond linker (Blue (B) rectangles) and the *N*,*N*-dimethylaminopropyloxy chain (Black (D) rectangle). Each of the four regions was modified systematically in order to assess structure-activity relationships (SARs). The compounds developed in each series were tested to obtain EC_{50} and E_{max} values. All modifications to aromatic ring A tested (Figure 3A), including the introduction of electron withdrawing or electron donating substituents, led to a reduction in activity compared to compound OX03771 (EC_{50}: 39 nM, E_{max}: 5).

To alter the three-dimensional shape of the molecule the alkane, alkyne and (*E*,*E*)-1,3-butadiene linker analogues were synthesised (Figure 3B), thereby varying either the compound's conformational flexibility, the relative orientation of or distance between the two aryl units. A secondary amide analogue was also prepared as an isostere of the (*E*)-alkene. Compound OX03384, which contains a fully saturated alkyl linker group, alkyne OX03383 and butadiene OX03385 all resulted in lower potency suggesting that the geometrical constraints imparted by the (*E*)-olefin are important. Compound OX03386, containing a secondary amide linker also showed much lower potency. Given the previously reported propensity of olefins to undergo metabolic oxidation reactions (Dharwadkar 2016), it was also of interest to investigate bicyclic isosteres OX03390-93, some of which may be anticipated to be more metabolically stable. Quinoline OX03390, quinoxaline OX03391 and benzofuran OX03392 all showed a reduction in potency compared to compound OX03771. Encouragingly

JPET Fast Forward. Published on March 30, 2017 as DOI: 10.1124/jpet.116.239574
This article has not been copyedited and formatted. The final version may differ from this version.

however, benzothiazole OX03393 showed only a modest drop in potency compared to compound OX03771, and a similar E_{max}.

Altering the regiochemistry within aromatic ring C was found to have a profound effect on the potency: both ortho and meta *N*,*N*-dimethylaminopropyloxy substituted analogues, compounds OX03394 and OX03373, showed a complete loss of activity (Figure 3C). Compound OX03387 suggested that reducing the electron density of aromatic ring C through introduction of an additional fluoro substituent resulted in reduced activity.

Finally the *N*,*N*-dimethylaminopropyloxy chain was modified as shown in Figure 5D. Hydroxyaryl derivative, compound OX03395, lacking the *N*,*N*-dimethylaminopropyl side chain showed a reduction in potency (EC_{50} = 3000 nM). The mono-methyl substituted counterpart (compound OX03389) gave an apparent modest drop in potency (EC_{50} = 320 nM) compared to compound OX03771, whereas the truncated homologue (compound OX03388) showed a significant reduction in potency (EC_{50} = 2000 nM). Compound OX03050, containing a propyl alcohol chain gave a comparable EC_{50} of 26 nM compared to 39 nM (compound OX03771) and a six-fold higher E_{max}, while both the *O*-methyl ether analogue (compound OX03374, EC_{50} = 1500 nM) and the alkyl substituted analogue (compound OX03373, EC_{50} = 1000 nM) showed a reduction in activity. Given that, under the assay conditions, the amines would exist predominantly as their corresponding ammonium salts, taken together these data suggest that the presence of a hydrogen bond donor within the side chain may confer higher levels of potency.

Compound OX03050 alongside other analogues that were thought may improve the *in vitro* ADME profile were incubated with mouse liver microsomes and their metabolic conversion measured over time (Figure 3E). Of these, compound OX03050 demonstrated the greatest metabolic stability, having a half-life greater than 45 minutes. All the other compounds tested had dropped below 5% of their starting amount by 45 minutes, so with the greatest potency and best *in vitro* metabolic stability profile compound OX03050 was taken forward for *in vivo* testing.

Compound OX03050 is able to drive the human *LDLR* promoter *in vivo*

To test whether the ADME profile seen in mouse liver microsomes was confirmed *in vivo*, an HPLC assay was developed to measure compound OX03050 in mouse plasma. 40 mg/kg of compound OX03050 was delivered via the intraperitoneal route (I.P) to CD-1 male mice and plasma taken at various time points up to 6 hours (Figure 4A). Compound OX03050 demonstrated a half-life of 84 minutes *in vivo*, consistent with the *in vitro* stability data, and could be detected at least up to 6 hours after dosing. To test the pharmacodynamic effects of Compound OX03050 *in vivo*, MF-1 male mice had a hydrodynamic injection of the p*LDLR-Luc* plasmid, in order to quantify *LDLR* promoter activity *in vivo* by non-invasive bioluminescence imaging. Baseline images were obtained five days after injection of the p*LDLR-Luc* plasmid (Figure 4C). Mice then received three doses of either vehicle, compound OX03050 (40 mg/kg) or pravastatin (600 mg/kg) spaced over 48 hours before final luciferase imaging (Figure 4C). An uninjected group which received the p*LDLR-Luc* plasmid but no I.P injections was used as a negative control. Compound OX03050 injected mice had significantly higher luciferase expression post compound delivery compared with vehicle treated mice (Figure 4B). Pravastatin injected mice also had significantly higher luciferase

JPET Fast Forward. Published on March 30, 2017 as DOI: 10.1124/jpet.116.239574
This article has not been copyedited and formatted. The final version may differ from this version.

expression than vehicle injected mice, as would be expected and has previously been shown (Hibbitt et al. 2010). No difference was observed between uninjected mice and mice receiving the vehicle treatment. Here we demonstrate that compound OX03050 is able to drive expression of the human *LDLR* promoter *in vivo*.

Compound OX03050 and compound OX03771 inhibit squalene synthase

We next confirmed that compound OX03771 upregulates the LDLR through a mechanism distinct from statins (Figure 5A). The activity of purified HMGCR is measured indirectly through measuring the absorption of NADPH at 340 nm over time. As HMGCR converts HMG-CoA to mevalonate, NADPH, a co-substrate in the reaction is oxidised to $NADP^+$, leading to a decrease in the absorption at 340 nm. The activity of the enzyme was confirmed, as there is a significant decrease in absorption between blank (no enzyme added) and vehicle treated samples (enzyme added). Pravastatin was used a positive control, which significantly inhibited the decrease in absorption compared to a vehicle treated sample after 15 minutes. No significant difference was observed between compound OX03771 and vehicle treated samples (Figure 5A), demonstrating that compound OX03771 does not exert its effects on LDLR expression *via* inhibition of HMGCR.

Squalene synthase activity was then measured in human liver microsomes in the presence of compounds OX03050 and OX03771. The compounds were pre-incubated with the microsomes for 10 minutes before the reaction was started by adding [^{3}H]-FPP. The reaction went on for 10 minutes before inhibition was assessed. The EC_{50} values for compound OX03050 (26 nM) and compound OX03771 (39 nM) established in the CHO-p*LDLR-Luc* assay and concentrations 10-fold above and below this were

used. Compounds OX03050 and OX03771 both inhibited the conversion of FPP to squalene in a dose-dependent manner, with both showing ~60% inhibition at the higher dose (Figure 5B). This suggests that the increase in LDLR expression observed with both compounds OX03050 and OX03771 is mediated, at least in part, by inhibition of squalene synthase.

In silico modelling was carried out on these compounds in an effort to rationalise their inhibitory potencies against squalene synthase. MOE software was used with the available human squalene synthase crystal structure (PDB: 1EZF), which had been co-crystallised with the ligand CP-320473 (Pandit *et al.* 2000). Compound OX03771 was docked in both its neutral state and as the corresponding protonated ammonium species for comparison. It was anticipated that OX03371 would exist predominantly as the protonated form under physiological conditions, but it was unclear which form would preferentially bind to squalene synthase. Docking studies were conducted as 30 independent experiments. For the ammonium salt of OX03771 no consistent docking prediction was found. In contrast, all solutions for the free base of OX03771 were predicted to bind in a similar manner to the ligand CP-320473 in the active site, with the hydrophobic aryl group sitting deep in the pocket while the chain bearing the hydrogen bond acceptor amino group was predicted to protrude out to interact with Arg-77 (Figure 5C). To further explore this putative interaction, compound OX03994 was docked into the active site, a molecule which demonstrated no activity in the CHO-p*LDLR-Luc* assay (Supplementary Figure 3). As with OX03771, the amino group within OX03994 is predicted to interact with Arg-77 however the molecule is predicted to adopt an alternative orientation within the active site as the regiochemistry of the *N*,*N*-dimethylaminopropyloxy substituent is switched from the para to meta. It is

possible that this leads to greater instability of the complex, which could explain the lack of activity observed for this compound. Compound OX03050 was predicted to bind in a similar manner to compound OX03771 (Figure 4D). As with the previous compounds the hydrophobic aryl group was predicted to insert into the active site pocket, however in a slightly different conformation with the terminal hydroxyl group predicted to interact with Arg77 and Tyr 72. The squalene synthase activity assay coupled with the *in silico* modelling provides a potential rationale to support compound OX03050 and OX03771 as inhibitors of squalene synthase.

A squalene synthase inhibitor and a statin in combination causes a synergistic drive in expression of the LDLR

We sought to determine if a squalene synthase inhibitor and statin used in combination are able to drive higher levels human *LDLR* promoter expression in a synergistic manner. The CHO-p*LDLR-Luc* cell line was treated with compounds for 48 hours to evaluate the effect of these small molecules in combination to drive the human *LDLR* promoter. A dose-response curve was generated for compound OX03050 (Figure 6A) and Simvastatin (Figure 6B) alone, giving EC_{50} values of 26 and 128 nM, respectively. A dose-response of compound OX03771 was carried out in the presence of compound OX03050 dosed at its EC_{50} (Figure 6C). There was no enhancement in luciferase activity using two squalene synthase inhibitors (E_{max}: 2.43 RLU/mg/mL) compared to the dose response of compound OX03771 alone (E_{max}: 3.28 RLU/mg/mL) (Figure 2A). The same effect was seen when two statins were dosed together, a dose response of pravastatin was carried out in the presence of Simvastatin dosed at its EC_{50} (Figure 6D). No increases in the luciferase activity were seen using two statins (E_{max}: 2.04 RLU/mg/mL) compared to Simvastatin alone (E_{max}: 2.76 RLU/mg/mL).

JPET Fast Forward. Published on March 30, 2017 as DOI: 10.1124/jpet.116.239574
This article has not been copyedited and formatted. The final version may differ from this version.

However, dose-response curves for Simvastatin in the presence of compound OX03050 dosed at its EC_{50} (Figure 6E) and EC_{80} (Figure 6F) gave a much greater increase in luciferase activity, giving E_{max} values of 6.35 and 11.77 RLU/mg/mL, respectively, than compared to two statins alone. The same was also true for the reverse experiment where a dose-response of compound OX03050 was carried out in the presence of Simvastatin dosed at its EC_{50} (Figure 6G). The E_{max} value was 16.77 RLU/mg/mL, a much larger increase in luciferase activity than seen using two squalene synthase inhibitors in combination. The fold increases in activity given when two squalene synthase inhibitors or two statins were dosed compared to vehicle treated cells was 3.9 and 1.1, respectively. In comparison, the fold increase when a statin was dosed alongside a squalene synthase inhibitor was 10- and 16.1-fold increase compared to vehicle treated cells. This is consistent with a synergistic effect of inhibiting the cholesterol biosynthesis pathway at two distinct parts of the pathway can greatly enhance the expression of the human *LDLR*.

JPET Fast Forward. Published on March 30, 2017 as DOI: 10.1124/jpet.116.239574
This article has not been copyedited and formatted. The final version may differ from this version.

Discussion

Here we present a novel series of small molecules able to upregulate LDL receptor expression (LDLR) through inhibition of squalene synthase. We first identified compound OX03771 from a focused small compound screen (216 molecules) in a reporter cell line produced in our laboratory. The reporter line contains a 10 kb human *LDLR* promoter element, including all components required for physiological regulation of expression, driving luciferase. The initial hit OX03771 was then confirmed in two secondary assays, and shown to increase LDLR expression at both the mRNA and protein level. Through systematic SAR studies we identified an even more potent analogue of compound OX03771 with improved *in vitro* metabolic stability, compound OX03050. We dosed compound OX03050 in mouse, establishing a pharmacokinetic profile of the drug and demonstrated that the efficacy seen *in vitro* translates to an *in vivo* system. Furthermore, we utilised a unique approach to quickly assess if compound OX03050 can drive the human LDLR promoter in a mammalian system. Delivery of the reporter vector via hydrodynamic delivery (a well-established method to deliver plasmid DNA directly to the liver (Liu, Song and Liu 1999)) resulted in an efficient and quick way to assess *in vivo* efficacy of our small molecules.

We next elucidated the mechanism of action of compounds OX03771 and OX03050 as inhibiting the enzyme squalene synthase, the first committed step in cholesterol biosynthesis. This suggests that the increase in LDLR expression observed with both compounds OX03050 and OX03771 is mediated, at least in part, by inhibition of squalene synthase. Other inhibitors of squalene synthase have previously been

reported and investigated for their effects on lipid-lowering (Elsayed and Evans 2008). Some of our small molecules resemble a series of stilbene derivatives reported several years ago as inhibitors of squalene synthase with modest potencies (Harwood *et al.* 1997). All the examples described by Harwood et al incorporate a basic amino group within the side chain appended to the stilbene and in their study and propose that the corresponding ammonium derivatives act as structural mimics of the cationic intermediate produced within the enzyme active site upon farnesyl pyrophosphate dimerization. Intriguingly, our compounds retain inhibitory potency even in the absence of an amino group in the side chain, e.g. OX03050 shows similar potency to OX03371, and our modelling studies predict similar interactions between protein and inhibitor for both compounds. Our small molecules share some similarity in structure to cholesterol so it is possible that they may also interact with other enzymes downstream of squalene synthase; however, this would have to be further investigated. Finally, we provided data to support that a squalene synthase inhibitor used in conjunction with a statin acts synergistically to increase LDLR expression.

In the future, our *in vivo* reporter model could be used to screen further arrays of small molecules for their ability to drive the human *LDLR* promoter in a mammalian system. This platform provides a quick and simple method to eliminate any compounds which fail to carry *in vitro* efficacy to an *in vivo* system. It is well known that statins do not have the same effect in rodents as they show in man, with studies showing a decrease in LDLR expression and no change in total cholesterol (Rashid *et al.* 2005) after statin administration. This in part could be attributed to the difference in how rodents and humans carry their cholesterol (Camus *et al.* 1983), with mice carrying most of their cholesterol in the high-density lipoprotein (HDL) fraction. Other differences due to the

absence of certain proteins such as cholesteryl ester transfer protein (Guyard-Dangremont *et al.* 1998) in mouse or inclusion of Apolipoprotein-4 8 (Greeve *et al.* 1993) into LDL particles result in a decreased shuttling of cholesterol ester to the LDL particles and enhanced clearance of LDL particles respectively. Inhibitors of cholesterol biosynthesis only consistently show efficacy in larger mammals, such as guinea pig (Matsunaga *et al.* 1991) or rabbit (Krause and Newton 1995). Our reporter system could provide a more economical and higher throughput platform to assess *in vivo* efficacy before embarking on a longer-term efficacy study in a larger animal model.

As lipid goals become stricter for patients who have dyslipidaemia, especially in high risk patients, such as those with heterozygous familial hypercholesterolaemia (heFH), high dose statins may become intolerable. Many studies have shown that only a small percentage of heFH patients reach their lipid goal (Pijlman *et al.* 2010). The emergence of the proprotein convertase subtilisin/kexin type 9 (PCSK9) inhibitors are a welcome addition to try and further lower the LDL-cholesterol of heFH patients (Robinson *et al.* 2015). The excellent lipid lowering seen with this class of biologics are surely promising however as they need to be administered via a subcutaneous injection every two weeks and are expected to have a high cost (Zimmerman 2015), an oral medication which can be taken alongside lower dose statins may still be of great use. We demonstrated that a squalene synthase inhibitor with a statin could cause a greater upregulation of *LDLR* promoter activity than can be achieved with either class of drug alone. Therefore, a lower dose of both classes of drugs could be used in high risk patients who are unable to tolerate maximal dose statins, hopefully alleviating the side effects they are experiencing. This enhanced efficacy has been

shown in the clinic previously (Stein *et al.* 2011) however the liver side effects seen with the squalene synthase inhibitor may mean a statin will have to be used alongside any squalene synthase inhibitor to inhibit a build-up of FPP (Wasko *et al.* 2011). Squalene synthase inhibitors have also been shown to lower triglycerides (Ugawa *et al.* 2000) which may be explained by recent studies investigating the orthologs differentially affected by squalene synthase inhibitors and statins (Rondini *et al.* 2016). Only squalene synthase inhibitors were shown to alter cellular lipid metabolism and so may provide another added benefit to using them alongside a statin.

Here, we have characterised a novel series of small molecules, the most active of which have potency in the nanomolar range. To further evaluate whether these compounds can lower LDL-cholesterol in an animal model, dosing a large animal model such as the guinea pig or rabbit model. These larger species share a similar lipid profile to humans, in which the majority of cholesterol is carried in the LDL-fraction and cholesterol levels respond to compounds which inhibit the cholesterol biosynthesis pathway. This further assessment will be critical for the progression of this series of molecules towards any future therapy.

Authorship contributions

Participated in research design: Kerr, Tam, Hibbitt, Hale, Douglas, Bataille, Wynne, Channon, Russell and Wade-Martins.

Conducted experiments: Kerr, Tam, Hale, Cioroch, Douglas, Agkatsev, Hibbit, Mason, Holt-Martyn and Bataille.

Performed data analysis: Kerr, Tam, Agkatsev, Mason, Holt-Martyn, Bataille, Wynne Russell, Channon and Wade-Martins.

Wrote or contributed to the writing of the manuscript: Kerr, Douglas, Wynne, Channon, Russell and Wade-Martins

References

Amin D, Cornell S a, Gustafson SK *et al.* Bisphosphonates used for the treatment of bone disorders inhibit squalene synthase and cholesterol biosynthesis. *J Lipid Res* 1992;**33**:1657–63.

Bitzur R, Cohen H, Kamari Y *et al.* Intolerance to Statins: Mechanisms and Management. *Diabetes Care* 2013;**36**:S325–30.

Camus M, Chapman MJ, Forgez P *et al.* Lipoproteins and Apoproteins in the Mouse ,. 1983;**24**.

Davidson MH. Squalene synthase inhibition: A novel target for the management of dyslipidemia. *Curr Atheroscler Rep* 2007;**9**:78–80.

Dharwadkar SS. Review Implications of Drug Metabolizing Enz Chemistry & Biology Interface. 2016.

Elsayed RK, Evans JD. Emerging lipid-lowering drugs: squalene synthase inhibitors. *Expert Opin Emerg Drugs* 2008;**13**:309–22.

Greeve J, Altkemper I, Dieterich JH *et al.* Apolipoprotein B mRNA editing in 12 different mammalian species: hepatic expression is reflected in low concentrations of apoB-containing plasma lipoproteins. *J Lipid Res* 1993;**34**:1367–83.

Guyard-Dangremont V, Desrumaux C, Gambert P *et al.* Phospholipid and cholesteryl ester transfer activities in plasma from 14 vertebrate species. Relation to atherogenesis susceptibility. *Comp Biochem Physiol - B Biochem Mol Biol* 1998;**120**:517–25.

Harwood HJ, Barbacci-Tobin EG, Petras SF *et al.* 3-(4-chlorophenyl)-2-(4-diethylaminoethoxyphenyl)-A-pentenonitrile monohydrogen citrate and related analogs. Reversible, competitive, first half-reaction squalene synthetase inhibitors. *Biochem Pharmacol* 1997;**53**:839–64.

Hibbitt OC, McNeil E, Lufino MM *et al.* Long-term physiologically regulated expression of the low-density lipoprotein receptor in vivo using genomic DNA mini-gene constructs. *Mol Ther* 2010;**18**:317–26.

Ichikawa M, Ohtsuka M, Ohki H *et al.* Discovery of DF-461, a potent squalene synthase inhibitor. *ACS Med Chem Lett* 2013;**4**:932–6.

Krause BR, Newton RS. Lipid-lowering activity of atorvastatin and lovastatin in rodent species: triglyceride-lowering in rats correlates with efficacy in LDL animal models. *Atherosclerosis* 1995;**117**:237–44.

Liu F, Song Y, Liu D. Hydrodynamics-based transfection in animals by systemic administration of plasmid DNA. *Gene Ther* 1999;**6**:1258–66.

Lusis AJ. Insight Review Articles. *Nature* 2000;**407**:233–41.

Marcoff L, Thompson PD. The Role of Coenzyme Q10 in Statin-Associated Myopathy. *J Am Coll Cardiol* 2007;**49**:2231–7.

Matsunaga A, Sasaki J, Takada Y *et al.* Effect of simvastatin on receptor mediated metabolism of low density lipoprotein in guinea pigs. 1991;**90**:31–7.

Moßhammer D, Schaeffeler E, Schwab M *et al.* Mechanisms and Assessment of Statin-related Muscular Adverse Effects. *Br J Clin Pharmacol* 2014:n/a-n/a.

Nagashima S, Yagyu H, Tozawa R *et al.* Plasma cholesterol-lowering and transient liver dysfunction in mice lacking squalene synthase in the liver. *J Lipid Res* 2015;**56**:998–1005.

Nishimoto T, Amano Y, Tozawa R *et al.* Lipid-lowering properties of TAK-475, a squalene synthase inhibitor, *in vivo* and *in vitro*. *Br J Pharmacol* 2003;**139**:911–8.

Nishimoto T, Ishikawa E, Anayama H *et al.* Protective effects of a squalene synthase inhibitor, lapaquistat acetate (TAK-475), on statin-induced myotoxicity in guinea pigs. *Toxicol Appl Pharmacol* 2007;**223**:39–45.

Pandit J, Danley DE, Schulte GK *et al.* Crystal Structure of Human Squalene Synthase. *Biochemistry* 2000;**275**:30610–7.

Pedersen TR. Randomised trial of cholesterol lowering in 4444 patients with coronary heart disease: the Scandinavian Simvastatin Survival Study (4S). *Lancet* 1994;**344**:1383–9.

Pijlman AH, Huijgen R, Verhagen SN *et al.* Evaluation of cholesterol lowering treatment of patients with familial hypercholesterolemia: a large cross-sectional study in The Netherlands. *Atherosclerosis* 2010;**209**:189–94.

Rashid S, Curtis DE, Garuti R *et al.* Decreased plasma cholesterol and hypersensitivity to statins in mice lacking Pcsk9. *Proc Natl Acad Sci U S A* 2005;**102**:5374–9.

Robinson JG, Farnier M, Krempf M *et al.* Efficacy and safety of alirocumab in reducing lipids and cardiovascular events. *N Engl J Med* 2015;**372**:1489–99.

Rondini EA, Duniec-Dmuchowski Z, Cukovic D *et al.* Differential regulation of gene expression by cholesterol biosynthesis inhibitors that reduce (pravastatin) or enhance (squalestatin 1) nonsterol isoprenoid levels in primary cultured mouse and rat hepatocytes. *J Pharmacol Exp Ther* 2016;**1**:216–29.

Shepherd J, Cobbe S, Ford I *et al.* Prevention of Coronary Heart Disease With Pravastatin in Men With. *Lancet (London, England)* 1995;**333**.

Sniderman AD, Lawler PR, Williams K *et al.* The causal exposure model of vascular disease. *Clin Sci (Lond)* 2012;**122**:369–73.

Stein E a., Bays H, O'Brien D *et al.* Lapaquistat acetate: Development of a squalene synthase inhibitor for the treatment of hypercholesterolemia. *Circulation* 2011;**123**:1974–85.

Thorne N, Shen M, Lea WA *et al.* Firefly luciferase in chemical biology: a compendium of inhibitors, mechanistic evaluation of chemotypes, and suggested use as a reporter. *Chem Biol* 2012;**19**:1060–72.

Ugawa T, Kakuta H, Moritani H *et al.* YM-53601, a novel squalene synthase inhibitor, reduces plasma cholesterol and triglyceride levels in several animal species. *Br J Pharmacol* 2000;**131**:63–70.

Wasko BM, Smits JP, Shull LW *et al.* A novel bisphosphonate inhibitor of squalene synthase combined with a statin or a nitrogenous bisphosphonate in vitro. *J Lipid Res* 2011;**52**:1957–64.

Zimmerman MP. How do pcsk9 inhibitors stack up to statins for low-density lipoprotein cholesterol control? *Am Heal Drug Benefits* 2015;**8**:436–42.

Footnotes

The work was funded by the British Heart Foundation (BHF) through Project Grant PG/10/54/28460 to RW-M and KC, a Research Councils' UK Fellowship awarded to AR, a BHF Studentship to AK, and support from the Oxford BHF Centre for Research Excellence (RE/08/004)

JPET Fast Forward. Published on March 30, 2017 as DOI: 10.1124/jpet.116.239574
This article has not been copyedited and formatted. The final version may differ from this version.

Figure legends

Figure 1: Identification of novel small molecules which upregulate *LDLR* genomic DNA promoter activity.

A compound library of 216 small molecules was screened at a single concentration (20 µM) in a CHO-p*LDLR-Luc* cell line. Luciferase is under the control of 10 kb of genomic DNA upstream of the *LDLR* locus, including the promoter and elements essential for physiological regulation. (A) Three initial hits appeared to give an increase in luciferase expression compared to DMSO (0.1%) control treated cells. (B) The structure of compound 49 (OX03771), the most potent of the initial hits. (C) The structure of compound 49 (OX03771) and cholesterol showing their similarity in structure.

Figure 2: Compound OX03771 dose dependently increases the LDLR at the mRNA and protein level with an EC_{50} in the nanomolar range

(A) CHO-p*LDLR-Luc* cells were treated with compound OX03771, or vehicle control (0.1% DMSO) for 48 hours before luciferase expression was measured. Compound OX03771 gave a dose dependent increase in luciferase expression compared with vehicle treated cells and had an EC_{50} in the nanomolar range. Luciferase expression was normalised to total protein; n=4 (**B**) Hep3B cells were treated with increasing doses of compound OX03771 for 24 hours before mRNA expression was analysed. Cholesterol treated (25.8 µM) and Simvastatin treated (500 nM) cells acted as a negative and positive control respectively. Compound OX03771 gave a significant increase in *LDLR* mRNA expression compared with vehicle treated cells; n=5. (**C**) Representative western blot and (**D**) quantification of mouse Hepa1-6 cells treated with increasing concentrations of compound OX03771 for 48 hours before Ldlr protein

expression was analysed. Cholesterol (25.8 µM) and Simvastatin (500 nM) were used as negative and positive controls respectively. Compound OX03771 gave a significant increase in Ldlr protein expression compared with vehicle cells; n=3. Error bars denote SD. Significance represents treatment compared to vehicle treated control. *P<0.05, **P<0.01, ***P<0.001. One-way ANOVA with Dunnett's post-hoc analysis.

Figure 3: Identification of compound OX03050 a more potent analogue of compound OX03771 with improved metabolic stability

Systematic SAR studies were carried out on compound OX03771, whereby each component of the molecule was altered individually and screened in the CHO-p*LDLR-Luc* at 1, 10, 30, 100, 300, 1000 and 10000 nM concentrations. The (**A**) red squared aromatic ring, (**B**) blue squared double bond linker, (**C**) purple squared aromatic ring and (**D**) N,N-dimethylaminopropyloxy chain modifications lead to the identification of compound OX03050, a compound with improved potency. All compounds were screened in duplicate. (**E**) Listed compounds were spiked into mouse liver microsomes and after given time points the remaining amounts were quantified through LC/MS. The amount is given in the table as a percentage in comparison with the amount detected at the 0 minute time point. Of these compound OX03050 was the most stable, with over half still present after 45 minutes.

Figure 4: Compound OX03050 is able to increase expression of the human *LDLR* promoter in a mammalian system

(**A**) Compound OX03050 (40 mg/kg) was detectable up to 6 hours post I.P administration in mouse plasma. (**B**) Timeline of *in vivo* efficacy study, p*LDLR-Luc* plasmid was delivered to MF-1 male mice via hydrodynamic injection on day 0. 5 days post hydrodynamic injection a (**C**) baseline image was taken for each mouse. Three

doses of either vehicle, compound OX03050 (40 mg/kg) or pravastatin (600 mg/kg) were administered over 48 hours before a second image was taken. An uninjected group where the plasmid was delivered but no compound was administered, was used as a negative control. (**D**) Compound OX03050 and pravastatin gave a significant increase in luciferase expression compared to vehicle treated mice. *P<0.05 n=5-6 per group, Error bars denote SEM. One-way ANOVA with Dunnetts post hoc analysis.

Figure 5: Compounds OX03771 and OX03050 competitively inhibit squalene synthase through binding in the active site.

(**A**) Purified HMGCR was added to samples containing either vehicle, pravastatin, compound OX03771, alongside all substrates necessary for the reaction to process. No enzyme added (Blank) and no compound added (Activity) samples acted as negative controls. Pravastatin significantly inhibited the decrease in absorbance at 340 nm, representing NADPH being oxidised to NADP+ and indicative of HMGCR activity. None of the other three compounds inhibited this decrease, demonstrating that they do not inhibit HMGCR; n=3. Error bars denote SD. (**B**) Purified human liver microsomes were incubated with radiolabelled FPP and all necessary co-substrates in the presence of compounds OX03771, OX03050 or vehicle. Both compounds OX03771 and OX03050 dose dependently inhibited squalene synthase activity at nanomolar concentrations; n=4-7. Error bars denote SEM. *In silico* modelling of (**C**) compound OX03771 and (**D**) OX03050 using MOE software. *P<0.05, ****P<0.0001.

Figure 6: A statin and squalene synthase inhibitor produce a synergistic effect further upregulating *LDLR* promoter activity

To determine if a statin and squalene synthase inhibitor produced a greater upregulation of the *LDLR* promoter dose response experiments in the CHO-p*LDLR*-

Luc cell line were carried out in the presence of the different cholesterol biosynthesis inhibitors. (**A**) A dose response of compound OX03050 and (**B**) simvastatin established the EC_{50} and EC_{80} values to be used in the combination treatments. (**C**) A dose response of compound OX03771 in the presence of the EC_{50} of compound OX03050, looking at the effect of two squalene synthase inhibitors. (**D**) A dose response of pravastatin in the presence of the EC_{50} of simvastatin, looking at the effect of two statins. (**E**) the EC_{50} and (**F**) EC_{80} of compound OX03050 treated alongside a dose response of simvastatin. (**G**) the EC_{50} of simvastatin treated alongside a dose response of compound OX03050. The dashed line represents vehicle (0.1% DMSO) treated cells and the dotted line is the single concentration of the EC_{50} or EC_{80} used as alongside. In combination using a statin and squalene synthase inhibitor leads to a much larger increase in luciferase expression than can be seen with two classes of the same inhibitor; n=4. Error bars denote SD.

JPET Fast Forward. Published on March 30, 2017 as DOI: 10.1124/jpet.116.239574
This article has not been copyedited and formatted. The final version may differ from this version.

Figure 1

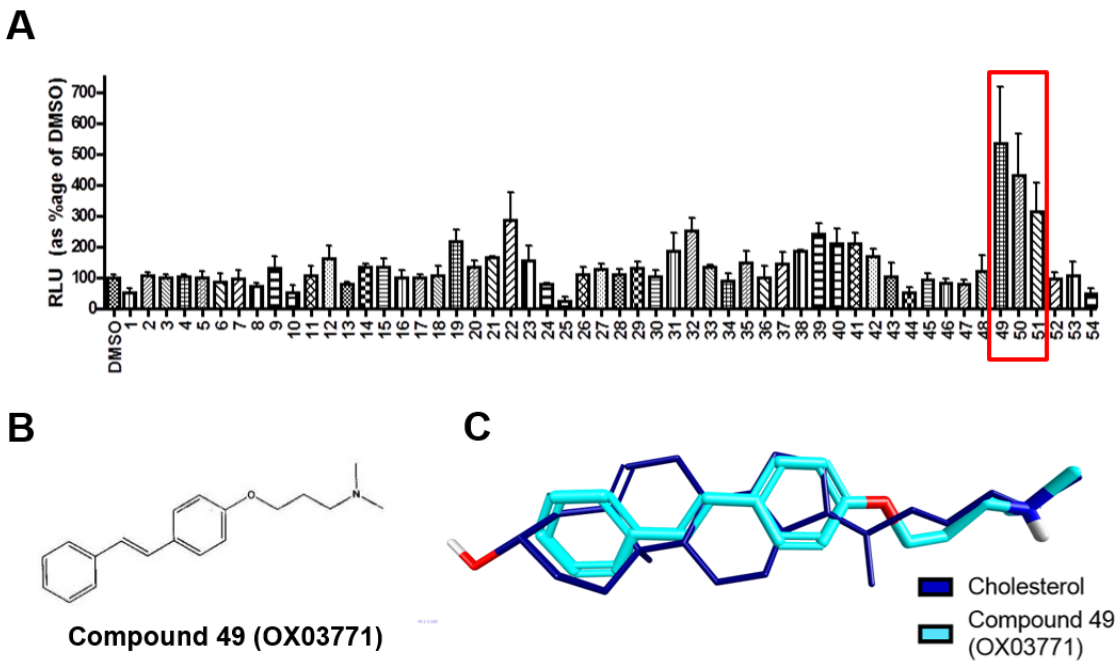

JPET Fast Forward. Published on March 30, 2017 as DOI: 10.1124/jpet.116.239574
This article has not been copyedited and formatted. The final version may differ from this version.

Figure 2

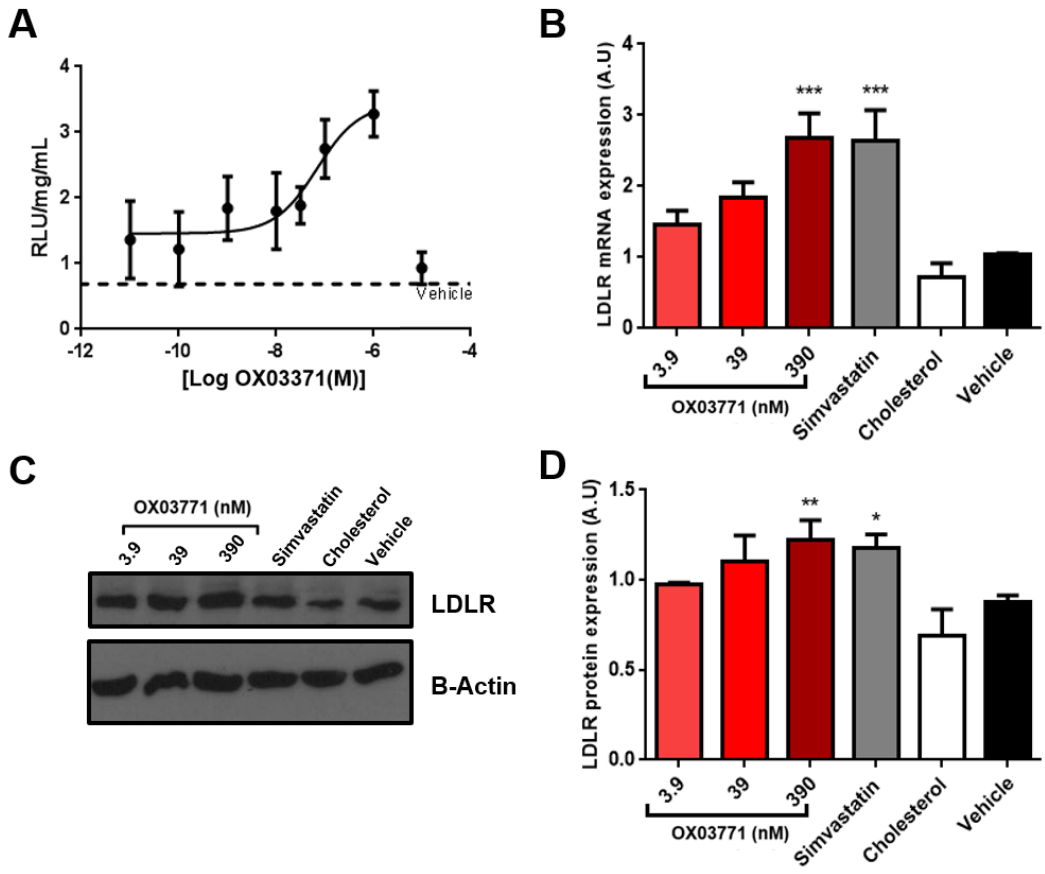

JPET Fast Forward. Published on March 30, 2017 as DOI: 10.1124/jpet.116.239574
This article has not been copyedited and formatted. The final version may differ from this version.

Figure 3

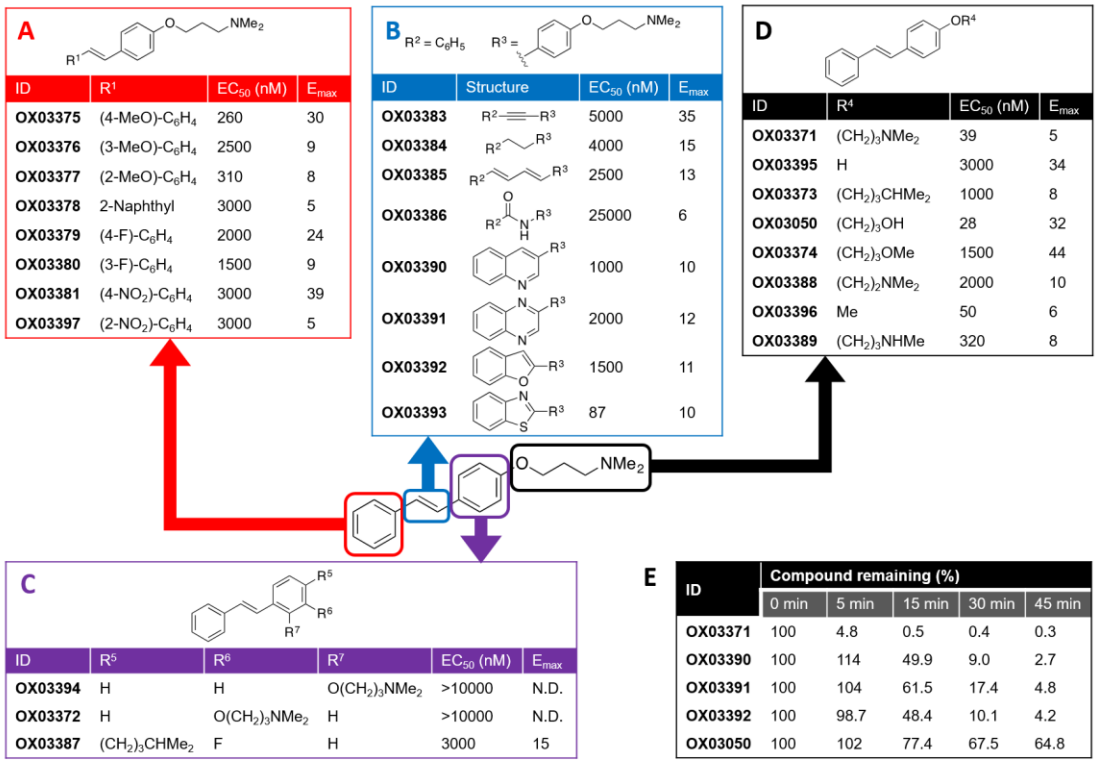

A

ID	R^1	EC_{50} (nM)	E_{max}
OX03375	(4-MeO)-C_6H_4	260	30
OX03376	(3-MeO)-C_6H_4	2500	9
OX03377	(2-MeO)-C_6H_4	310	8
OX03378	2-Naphthyl	3000	5
OX03379	(4-F)-C_6H_4	2000	24
OX03380	(3-F)-C_6H_4	1500	9
OX03381	(4-NO_2)-C_6H_4	3000	39
OX03397	(2-NO_2)-C_6H_4	3000	5

B

ID	Structure	EC_{50} (nM)	E_{max}
OX03383	R^2—≡—R^3	5000	35
OX03384	R^2—R^3	4000	15
OX03385	R^2—=—R^3	2500	13
OX03386	R^2—C(=O)—N(H)—R^3	25000	6
OX03390		1000	10
OX03391		2000	12
OX03392		1500	11
OX03393		87	10

C

ID	R^5	R^6	R^7	EC_{50} (nM)	E_{max}
OX03394	H	H	$O(CH_2)_3NMe_2$	>10000	N.D.
OX03372	H	$O(CH_2)_3NMe_2$	H	>10000	N.D.
OX03387	$(CH_2)_3CHMe_2$	F	H	3000	15

D

ID	R^4	EC_{50} (nM)	E_{max}
OX03371	$(CH_2)_3NMe_2$	39	5
OX03395	H	3000	34
OX03373	$(CH_2)_3CHMe_2$	1000	8
OX03050	$(CH_2)_3OH$	28	32
OX03374	$(CH_2)_3OMe$	1500	44
OX03388	$(CH_2)_2NMe_2$	2000	10
OX03396	Me	50	6
OX03389	$(CH_2)_3NHMe$	320	8

E

ID	Compound remaining (%)				
	0 min	5 min	15 min	30 min	45 min
OX03371	100	4.8	0.5	0.4	0.3
OX03390	100	114	49.9	9.0	2.7
OX03391	100	104	61.5	17.4	4.8
OX03392	100	98.7	48.4	10.1	4.2
OX03050	100	102	77.4	67.5	64.8

JPET Fast Forward. Published on March 30, 2017 as DOI: 10.1124/jpet.116.239574
This article has not been copyedited and formatted. The final version may differ from this version.

Figure 4

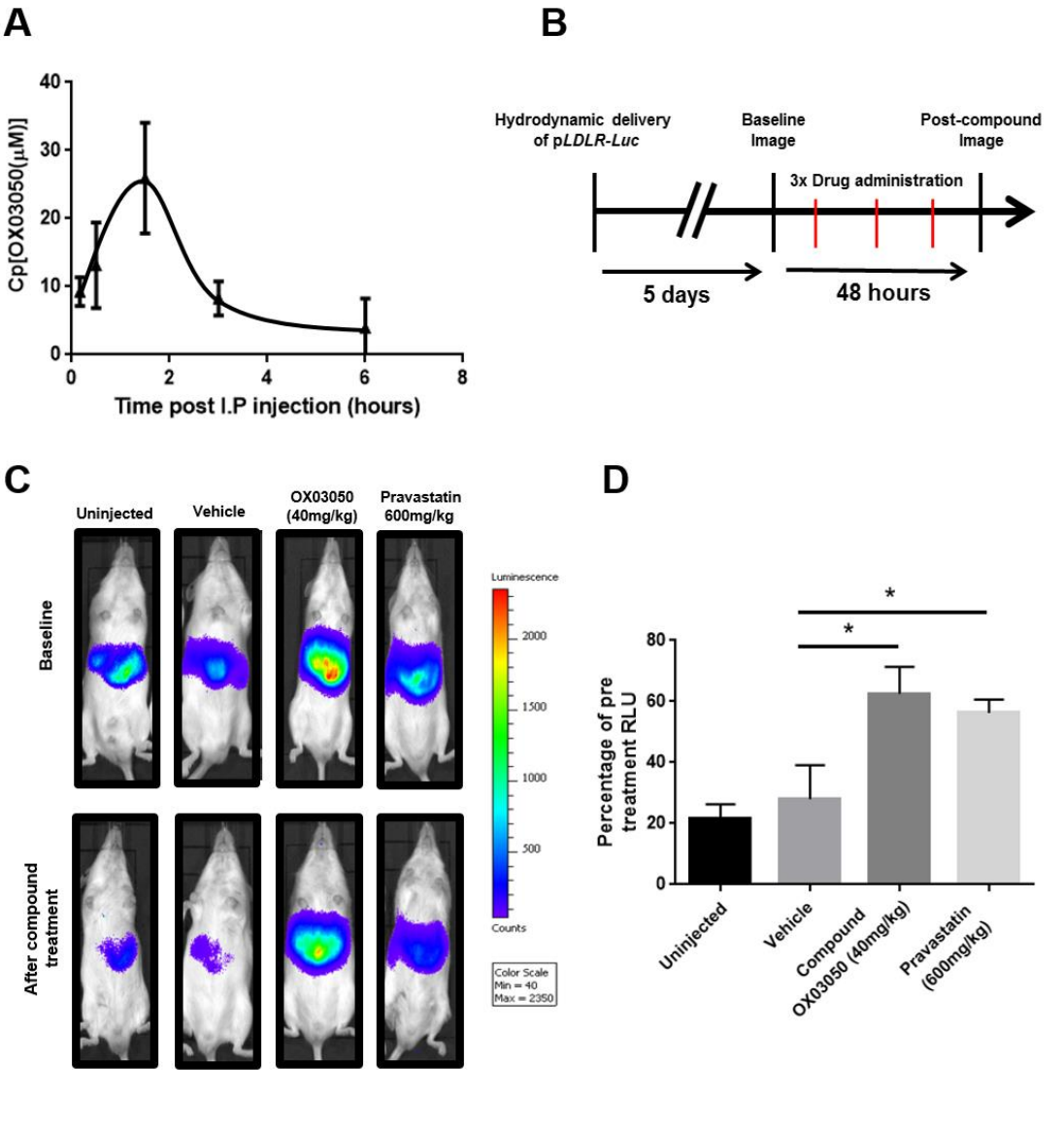

JPET Fast Forward. Published on March 30, 2017 as DOI: 10.1124/jpet.116.239574
This article has not been copyedited and formatted. The final version may differ from this version.

Figure 5

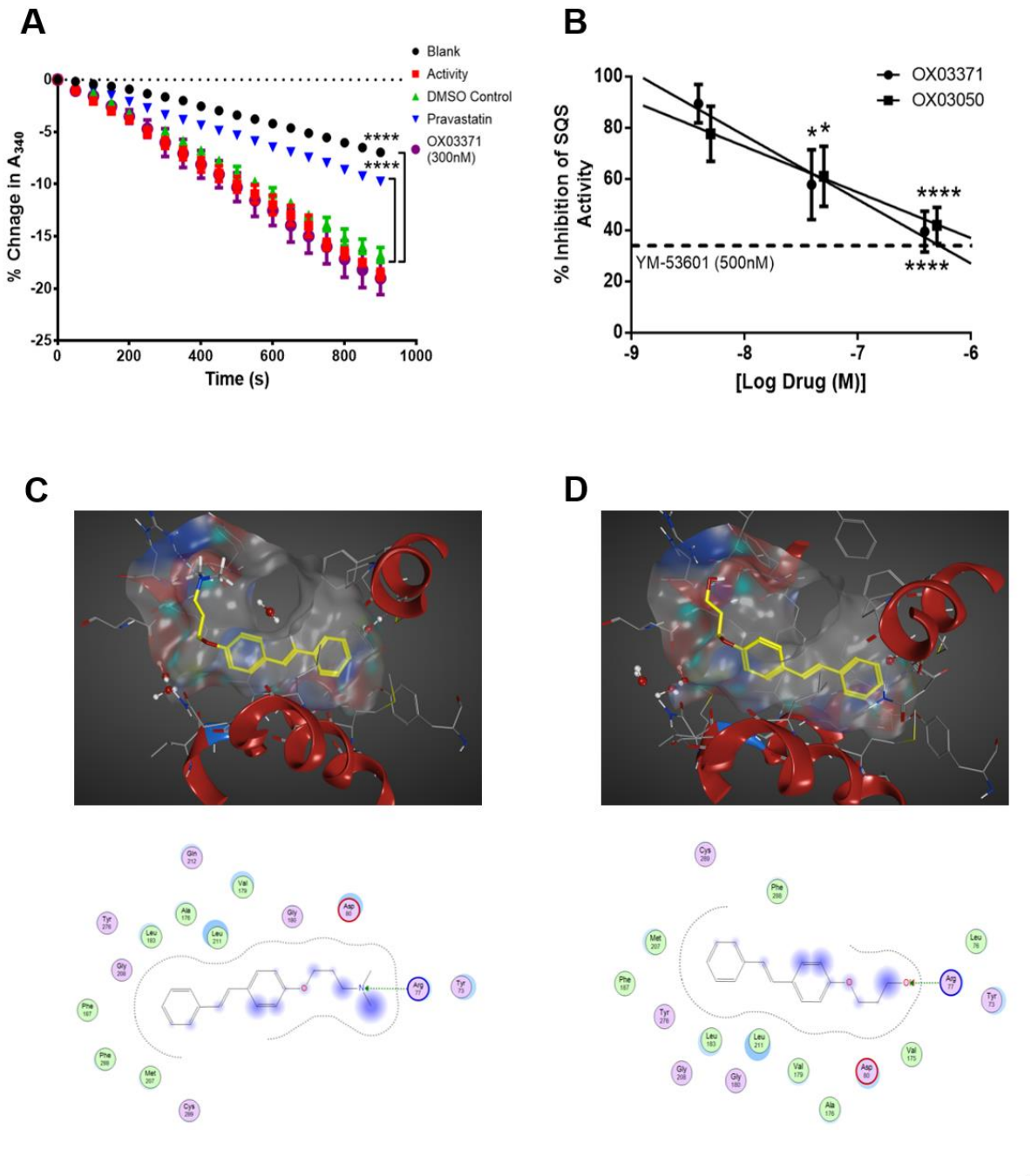

JPET Fast Forward. Published on March 30, 2017 as DOI: 10.1124/jpet.116.239574
This article has not been copyedited and formatted. The final version may differ from this version.

Figure 6